Dual Fabry–Perot filter for measurement of CO rotational spectra: design and application to the CO spectrum of Venus

E. Serabyn, D. J. Benford, S. Wu, and J. R. Pardo

We present the design of a harmonic resonant filter that can be used with a Fourier transform spectrometer (FTS) for simultaneous measurement of a series of lines in the CO rotational ladder. To enable studies of both broad CO absorptions in Venus and modestly red-shifted CO emission from external galaxies, relatively broad (approximately 10–30-GHz FWHM) transmission passbands are desirable. Because a single low-finesse Fabry–Perot (FP) etalon has insufficient interline rejection, a dual-FP etalon was considered. Such a design provides significantly better interband rejection and somewhat more flattopped transmission spikes. A prototype filter of this type, made of two thin silicon disks spaced by an air gap, has been constructed and used with our FTS at the Caltech Submillimeter Observatory for simultaneous measurement of the four submillimeter CO transitions in the atmosphere of Venus that are accessible from the ground.

OCIS codes: 300.6270, 300.6300, 350.1270, 050.2230.

1. Introduction

The most direct method of measuring wideband astronomical spectra at far-infrared wavelengths is Fourier transform spectroscopy.[1,2] However, the complete spectral coverage provided by this technique is not always optimal. For example, in the case of the rotational spectra of light linear molecules, which consist of a nearly harmonic series of narrow, widely spaced lines, the relevant spectral regions are regularly spaced, narrow windows. In the background-dominated regime the large interline background power entering a broadband Fourier transform spectrometer (FTS) will then limit the minimum detectable line flux. To optimize the signal-to-noise ratio (SNR) on a harmonic series of lines, a filter resonant at the same series of harmonic frequencies, such as a Fabry–Perot (FP) filter, would be apropos. FTS filtering for the cases of a single narrow passband,[3] and the simultaneous detection of a pair of lines with two FP orders,[4] has been previously considered. Here we point out that the harmonic nature of the FP transmission curve makes a FP filter an ideal match to the harmonic spectrum case. Specifically, we discuss the design and construction of a filter that is tailored to the detection of the CO rotational ladder at submillimeter wavelengths.

In astronomical sources ranging from the planet Venus to interstellar molecular clouds to distant galaxies, the molecular species with the strongest far-infrared and submillimeter lines is CO. However, multitransition observations remain difficult at long wavelengths, owing to the inherent mismatch between the widely spaced lines and the narrow-band (but sensitive and high-resolution) heterodyne receivers typically in use. In the case of Venus, additional complications include pressure-broadened line wings extending beyond the narrow heterodyne passbands available (so that the full structure of the CO line profiles in Venus has yet to be seen) and limited on-source time that is due to proximity to the Sun. Prior observations of Venus have thus been limited largely to the lowest two rotational transitions[5,6] ($J = 1$–0 and $J = 2$–1) and exclusively to the line cores. A broadband FTS can thus provide important complementary information: CO line integrals with a com-

E. Serabyn (gene.serabyn@jpl.nasa.gov), D. J. Benford, and J. R. Pardo are with the Department of Physics, California Institute of Technology, MC 320-47, Pasadena, California 91125. S. Wu is with the Department of Electrical Engineering, MC 136-36, California Institute of Technology, Pasadena, California 91125.

Received 25 January 2000; revised manuscript received 16 August 2000.

0003-6935/00/346448-05$15.00/0

mon calibration over a wide range of rotational quantum number, J.

Since published Venusian CO spectra all show strong line wings extending at least several hundred megahertz from line center, what is desired is a resonant filter of spacing equal to the CO line spacing (115.271 GHz), with a passband width many times the expected linewidth, or approximately 10–20 GHz. A second application of such a filter would be the measurement of CO emission spectra for galaxies with moderate recessional velocities. To allow for red shifts of several thousand kilometers/s, a useful bandwidth would be similar, of order 10–30 GHz. The desired filter finesse, f (the ratio of the resonance spacing to the transmission half-widths), is thus rather low, ≤ 10.

The level of out-of-band rejection is important, because even at high, dry sites, the atmosphere is semitransparent only up to frequencies of ~ 1 THz,[7] with at best approximately 50–70% transmission in the two major atmospheric windows above 500 GHz. Thus observations of CO lines only up to $J = 7$–6 are generally possible (and the atmosphere is completely opaque at the $J = 5$–4 frequency). The thermal background power on a broadband detector will then be large compared with the power in the filter passbands unless an out-of-band rejection of ≥ 10 is available.

2. Design

The simplest method of fabricating a FP etalon is to use a thin, plane-parallel slab of high-index, lossless dielectric. At the long wavelengths under consideration, a solid disk half a wavelength thick is practical, and the available high dielectric indices, n, provide for sizable single-surface power reflectivities [30% for silicon (Si) with $n = 3.4$, and 35% for germanium with $n = 3.9$].[8] However, the finesses[9] are only 2.46 and 2.86 in the two respective cases. For such low f values the out-of-band rejection is inadequate, reaching at best[9] $(n^2 + 1)^2/(4n^2)$, or factors of 3.4 and 4.3, respectively. A maximum interband rejection of a factor of 10 can only be achieved for $n = 6.16$, an impracticably large value.

Since reflective dielectric coatings are problematical at such long wavelengths, we instead considered the next-simplest case: a dual-FP etalon consisting of a series of two thin dielectric disks, separated by an air or vacuum gap. Such a dual FP might be expected to be adequate, because the square of the single-FP interband rejection maxima exceeds an order of magnitude. Because Si is a readily available material, has good submillimeter transmission properties, is relatively straightforward to etch, and has found previous use in a different type of longwave FP,[10] we focus hereafter solely on Si-based dual FP's.

The theory of the dual FP is established[11] and results in analytical expressions for simple cases such as an identical pair of FP etalons spaced by an air gap. To calculate the transmission as a function of frequency for an arbitrary dual FP, we instead used a numerical implementation of the standard multi-

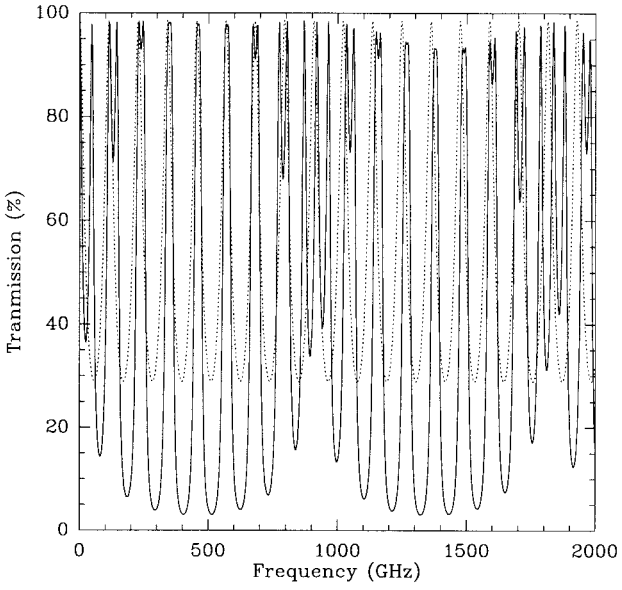

Fig. 1. Theoretical transmission of a single- (dotted curve) versus a dual- (solid curve) FP etalon, comprised of silicon disks of refractive index 3.42 and thickness 385 μm. The dual FP has a 140-μm air gap.

layer matrix formalism.[12] We began by assuming two identical etalons resonant at 115.271 GHz, which requires thicknesses of $d = 382.7$ μm. We can estimate the interetalon gap thickness by requiring a resonant frequency greater than the maximum frequency of interest, 1 THz. This calls for a gap width of <195 μm. Refinement of the model quickly yielded a satisfactory dual-FP design, whose transmission is compared with that of a single FP in Figs. 1 and 2. The final etalon design consists of two Si

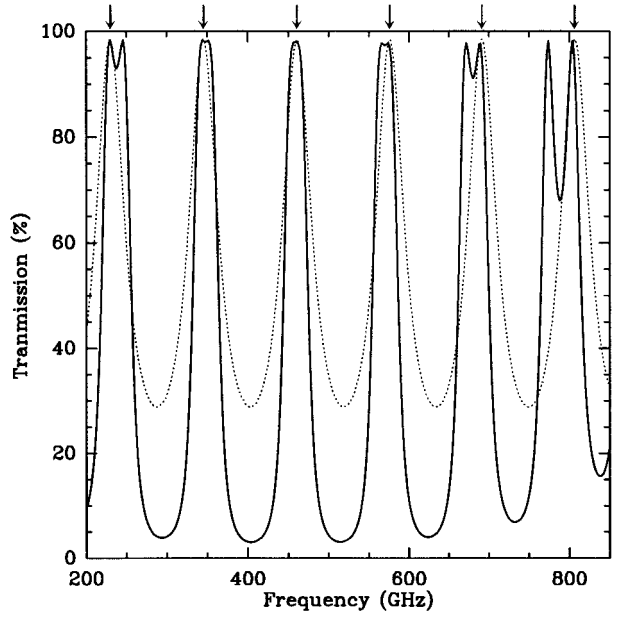

Fig. 2. Enlargement of Fig. 1 for the region of prime interest, with CO line positions labeled. Note the shift of the passbands relative to the CO line frequencies in the dual-etalon case.

disks of thickness 385.5 ± 1.0 μm spaced by a vacuum gap of 140 ± 10 μm. The allowable Si thickness error is determined by requiring a frequency error near 1 THz that is substantially smaller than the ~20-GHz passband bandwidth.

The period of the Airy-like variation in the transmission minima is dependent on the spacing between the two Si etalons. To optimize the out-of-band rejection for the frequencies of maximum interest (200–900 GHz), the vacuum gap must have a resonant frequency of 1100 ± 100 GHz. The calculated maximum out-of-band rejection is at best a factor of 30, ten times better than with a single etalon (Fig. 1). In the lowest six minima, the average maximum rejection ratio is 14, an improvement of roughly a factor of 5 from the single-etalon case (of course, the rejection ratio varies both across individual stop bands and from band to band).

As seen in Fig. 2, the passband half-widths are relatively unaffected in the region of interest, but the transmission profiles tend to be somewhat more flat-topped in the dual-FP case, also a desirable characteristic (albeit at the cost of some ringing, especially in the 800-GHz resonance). However, because of the interplay between resonances, the resonance centroids are no longer perfect multiples—in particular, a regular shift of the passband centroid frequencies with order number is evident. To alleviate this effect, the thicknesses were adjusted to place the highest-frequency CO line of interest ($J = 7$–6) to one side of its transmission resonance, and the lowest-frequency line of interest ($J = 2$–1) on the opposite side of its resonance, resulting in a regular shift of the resonance centroids relative to the CO lines across the region of interest.

3. Fabrication

We first acquired double-side–polished, 25-mm-diameter, Si wafers with a 100 orientation,[13] prethinned to a thickness of 390 ± 7 μm, slightly larger than desired so that the final thickness could be reached by etching. The two sides of each disk were parallel to 0.5 μm across the filter's final clear aperture. The thickness of each wafer was determined in two ways. First, the room-temperature transmission spectrum at wavelengths between 7 and 12 μm was measured with a commercial infrared FTS.[14] In this spectral region the refractive index is roughly[15] 3.42. More than 150 surface-reflection channel fringes were counted, allowing for the determination of the thickness to ≲0.05-μm absolute accuracy. The second method used a temperature-controlled Mahr Universal Measuring Machine[16] with an absolute accuracy of 0.24 μm and a relative accuracy of 0.12 μm. The latter permits the measurement of thickness variations to 300 parts in 10^6. The two sets of measurements were typically found to agree to within the measurement accuracies, although a few samples yielded inconsistencies.

The Si wafers were next thinned uniformly by growth and removal of a thermal oxide layer on the Si surface. First the Si disks were cleaned in a hydrogen peroxide and sulfuric acid solution at 120 °C. Next, an approximately 1.4-μm-thick layer of surface Si was converted to 3 μm of SiO_2 in a thermal oxidation furnace at 1050 °C for 18 h. Finally, the oxide was stripped away by buffered hydrofluoric acid, resulting in a slightly thinner, but still optically flat Si wafer. A second set of measurements indicated that 1.37 μm were removed from each side in one etching process. Several of the wafers were then chosen to be thinned one additional time. The final best wafers were again measured and found to be 384.8 and 386.4 μm thick, bracketing the desired 385.5-μm thickness to within the 1.0-μm tolerance.

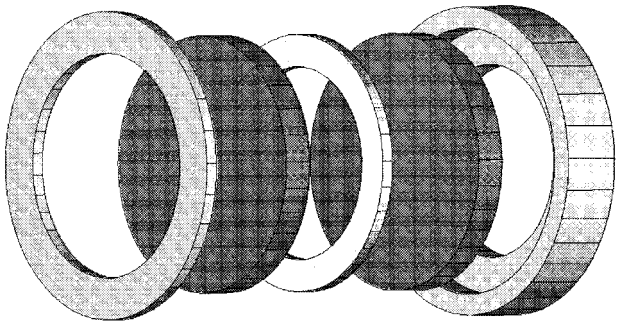

Fig. 3. Diagram of the FP layout. The component thicknesses have been substantially enhanced for clarity. The components are, from left to right, Be–Cu spring washer, Si disk (386-μm thick), stainless-steel spacer ring (140 μm), Si disk (385 μm), aluminum mounting cup.

The filter stack (Fig. 3) is comprised of the two Si disks spaced by a thin stainless-steel washer, nominally 140 μm thick. The stack is set in an aluminum cup for easy heat sinking, with a Be–Cu washer screwed into place above the filter stack to hold it in the cup with some spring loading to account for thermal contraction upon cooling to cryogenic temperatures. Because of the small component thicknesses, thermal contraction in the stack direction (a few tenths of a micrometer) is much less than the desired tolerance. The resultant clear aperture of the filter is ~2 cm in diameter.

4. Laboratory Measurements

The assembled filter was first installed in a filter wheel in a cryogenic Dewar with a bolometric detector operating at 1.5 K.[17] The detector viewed a chopped (150 Hz) hot–cold load through our submillimeter-wavelength laboratory FTS.[18] An aperture stop was placed in the collimated FTS beam, and an off-axis paraboloidal mirror near the Dewar window reimaged this aperture stop onto the filter inside the Dewar (where the beam was also collimated). The FTS was scanned ≈40 mm, yielding a spectral resolution of 4.5 GHz. Spectra with the CO filter in place and out of the beam were divided to derive absolute transmission. This procedure was carried out with two beam splitters optimized for 100–900 and 300–1600 GHz, respectively, and the two resulting spectra were averaged.

The measured transmission of the assembled filter

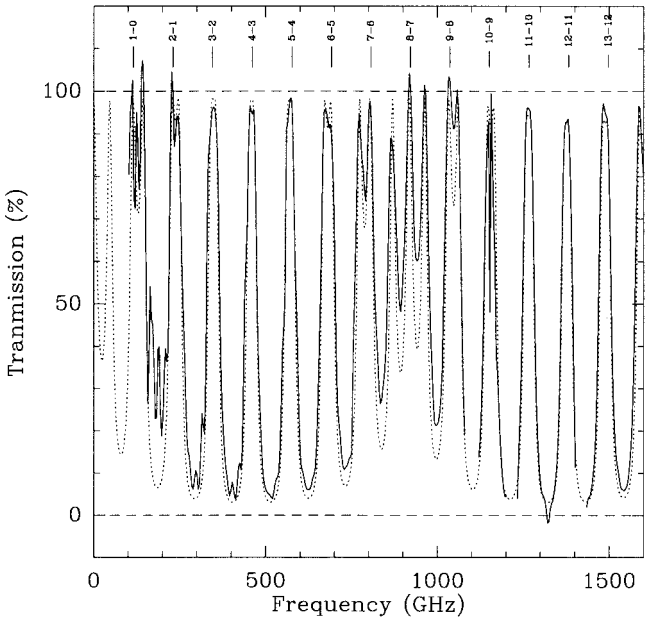

Fig. 4. Measured absolute filter transmission (solid curve) versus theoretical (dotted curve), with CO transitions labeled. The peak transmissions are >96%. The data below 150 GHz have been smoothed to account for the decreasing signal at longer wavelengths, and a few other regions of poor SNR have been blanked out.

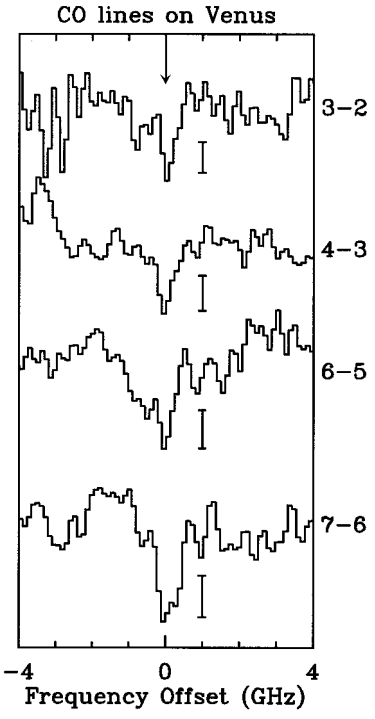

Fig. 5. Measured spectra of Venus in the vicinity of the four accessible CO lines. (The 5–4 and the 8–7 transitions are blocked by atmospheric water-vapor lines). The spectra have been divided by that of Jupiter. 10% absorption levels are indicated. The spectra are somewhat noisy, but all four spectra show a feature at the appropriate CO transition frequency.

is compared with the theoretical calculation in Fig. 4. After allowing for the index decrease[19] to $n = 3.382$ upon cooling to 1.5 K, the agreement is excellent in regions of high SNR: Fitting the dual-FP curve to our 1.5-K measurements yields $n = 3.385 \pm 0.010$ across 500–1500 GHz. However, the Airy-like variation in the transmission minima in Fig. 4 has a period of ~920 GHz instead of the design 1100 GHz. It may be that the distance between the Si disks is larger than planned, if, e.g., the spacer ring is not perfectly flat, but this is a large effect. The theoretical curve in Fig. 4 thus assumes an etalon spacing of 160 μm instead of 140 μm.

5. Initial Observations of Venus

The assembled filter was next installed in our FTS[2,20] at the Caltech Submillimeter Observatory on Mauna Kea, Hawaii, to observe Venus's CO absorption spectrum. Observations of Venus were carried out on the mornings of 1 and 2 April 1998. In the limited time available before sunrise it was possible to acquire only 16 high-resolution (220-MHz) on-source FTS scans. Shown in Fig. 5 are the sections of the resultant spectrum near the accessible CO lines in our 300–1000-GHz passband (the upper frequency bound is determined by the atmospheric cutoff and a 1.1-THz low-pass filter and the lower bound by the bolometer feed-horn cutoff). Absorption features of modest SNR (in the range of 3–6 σ) are present at all four of the CO transition frequencies. To our knowledge, the three high-frequency lines are first detections in Venus. Interpretation of these results will be presented elsewhere after further measurements, but it is already clear from these initial data that the measured line integrals are larger than is suggested by integrating over the line cores seen with narrow-band heterodyne receivers. The integrated line wings thus probe deeper into the atmosphere than do the line cores seen in previous observations of Venus.[5,6]

6. Conclusions

We have fabricated a dual Fabry–Perot (FP) resonant filter for astronomical use that selectively transmits the rotational transitions of CO below 1 THz, allowing for simultaneous measurement of a series of submillimeter CO transitions. For a source with strong CO lines, this filter thus allows for accurate calibration of CO relative line strengths.

The sensitivity of such a harmonically filtered system can be compared with a simple low-pass–filtered FTS covering the entire subterahertz domain and also with a narrow-band–filtered FTS limited to a single atmospheric window and CO line at a time. However, the complex spectrum of the background power (a Rayleigh–Jeans frequency rise modified by the H_2O-dependent atmospheric opacity curve[7]) leaves such comparisons less than straightforward. Nevertheless, in rough terms, the background power in the harmonic case is ~1 order of magnitude lower than in the low-pass case (allowing for the bandwidth reduction; the fact that the background power is pre-

dominantly from the high-frequency end of the band; and the fact that the background power arises predominantly in the opaque regions of the atmospheric spectrum, which are by design largely outside the filter resonances). Therefore we expect a SNR improvement over the low-pass case of a factor of ~3. However, the one-by-one approach to measuring the CO lines would provide a higher SNR for the lower-frequency lines, owing to the exclusion of the high-frequency background in that case, and a lower SNR on the higher-frequency lines, owing to the broader passband (≈100 GHz) of filters matched to atmospheric windows. In addition, the sequence of measurements would be of the order of a factor of 4 longer, because of the need for sequential measurements with associated time overheads. Of course, a line-by-line measurement approach defeats the basic goal of a common calibration with low systematic errors, and so the latter comparison is somewhat artificial.

This study was supported by NASA grant NAG5-6816. We thank G. R. Rossman for the use of his FTS and Y. C. Tai for access to etching facilities.

References

1. E. L. Wright, J. C. Mather, C. L. Bennett, E. S. Cheng, R. A. Shafer, D. J. Fixsen, R. E. Eplee, R. B. Isaacman, S. M. Read, N. W. Boggess, S. Gulkis, M. G. Hauser, M. Janssen, T. Kelsall, P. M. Lubin, S. S. Meyer, S. H. Moseley, T. L. Murdock, R. F. Silverberg, G. F. Smoot, R. Weiss, and D. T. Wilkinson, "Preliminary spectral observations of the galaxy with a 7° beam by the Cosmic Background Explorer (COBE)," Astrophys. J. **381,** 200–209 (1991).
2. E. Serabyn and E. W. Weisstein, "Fourier-transform spectroscopy of the Orion molecular cloud core," Astrophys. J. **451,** 238–251 (1995).
3. D. E. Jennings, D. Deming, G. R. Wiedemann, and J. J. Keady, "Detection of 12 micron Mg I and OH lines in stellar spectra," Astrophys. J. **310,** L39–L43 (1986).
4. M. F. Campbell, L. Haser, and S. Drapatz, "Fabry–Perot etalons as prefilters for astronomical far-infrared Fourier transform spectroscopy," Infrared Phys. **29,** 947–959 (1989).
5. R. T. Clancy and D. O. Muhleman, "Long-term (1979–1990) changes in the thermal, dynamical, and compositional structure of the Venus mesosphere as inferred from microwave spectral line observations of C-12O, C-13O, and CO-18," Icarus **89,** 129–146 (1991).
6. M. A. Gurwell, D. O. Muhleman, K. P. Shah, G. L. Berge, and D. J. Rudy, "Observations of the CO bulge on Venus and implications for mesospheric winds," Icarus **115,** 141–158 (1995).
7. E. Serabyn, E. W. Weisstein, D. C. Lis, and J. R. Pardo, "Submillimeter Fourier-transform spectrometer measurements of atmospheric opacity above Mauna Kea," Appl. Opt. **37,** 2185–2198 (1998).
8. J. W. Lamb, "Miscellaneous data on materials for millimetre and submillimetre optics," Int. J. Infrared Millim. Waves **17,** 1997–2034 (1996).
9. E. Hecht, *Optics* (Addison-Wesley, Reading, Mass., 1997), Chap. 9.
10. J. J. Bock, M. Kawada, H. Matsuhara, P. L. Richards, and A. E. Lange, "Silicon-gap Fabry–Perot filter for far-infrared wavelengths," Appl. Opt. **34,** 3651–3657 (1995).
11. G. Hernandez, *Fabry–Perot Interferometers* (Cambridge University Press, Cambridge, 1986).
12. M. Born and E. Wolf, *Principles of Optics* (Pergamon Press, London, 1959), Chap. 1.
13. Virginia Semiconductor, 1501 Powhatan Street, Fredericksburg, Va. 22401; telephone 540-373-2900.
14. Nicolet 60SX spectrometer, Nicolet Instruments, 5225 Verona Rd., Madison, Wis. 53711; telephone 800-232-1472.
15. E. D. Palik, ed., *Handbook of Optical Constants of Solids* (Academic, New York, 1983).
16. Accurate Instrument Repair, 1650-A N. Glassell St., Orange, Calif. 92667; telephone 714-637-5030.
17. Infrared Labs, 1808 East 17th St., Tucson, Ariz. 85719-6505; telephone 520-622-7074.
18. M. Bin, D. J. Benford, M. C. Gaidis, T. H. Büttgenbach, J. Zmuidzinas, E. Serabyn, and T. G. Phillips, "A large throughput high resolution Fourier transform spectrometer for submillimeter applications," Int. J. Infrared Millim. Waves **20,** 383–400 (1999).
19. E. V. Loewenstein, D. R. Smith, and R. L. Morgan, "Optical constants of far infrared materials. 2. Crystalline solids," Appl. Opt. **12,** 398–406 (1973).
20. E. Serabyn and E. W. Weisstein, "Calibration of planetary brightness temperature Spectra at near-millimeter and submillimeter wavelengths with a Fourier-transform spectrometer," Appl. Opt. **35,** 2752–2763 (1996).